Paper No. 89

CRASH IMPACT BEHAVIOUR OF SIMULATED COMPOSITE AND ALUMINIUM HELICOPTER FUSELAGE ELEMENTS

D.C. Bannerman

Deutsche Forschungs- und Versuchsanstalt
für Luft- und Raumfahrt e.V.
Stuttgart

U.S. Air Force, Visiting Scientist

- GERMANY -

and

C.M. Kindervater

Deutsche Forschungs- und Versuchsanstalt
für Luft- und Raumfahrt e.V.
Stuttgart
- GERMANY -

September 13-15, 1983
STRESA / ITALY

CRASH IMPACT BEHAVIOUR OF SIMULATED COMPOSITE

AND ALUMINIUM HELICOPTER FUSELAGE ELEMENTS

D.C. Bannerman*

and

C.M. Kindervater

Institut für Bauweisen- und Konstruktionsforschung

Deutsche Forschungs- und Versuchsanstalt
für Luft- und Raumfahrt e.V.
Stuttgart
- GERMANY -

ABSTRACT

An experimental investigation was conducted to study
the crash impact behaviour of simple helicopter structural
elements in order to provide some of the basic knowledge re-
quired for designing to crashworthiness specifications.
Aluminium tubes of circular and square cross sections having
thickness to diameter ratios between .01 and .10 as well as
aluminium and composite beam sections of stringer stiffened
and sandwich constructions were examined under quasi-static
and impact conditions. Speeds at impact were varied up to
12.8 m/s in accordance with MIL-STD-1290. The basic energy
absorption characteristics - crush load uniformity, speci-
fic energy, crush stroke efficiency, and average crush stress -
are discussed and compared. The influence of impact velocity
along with failure modes and the effects of trigger mecha-
nisms used to help initiate stable and efficient crushing
actions are also discussed.

INTRODUCTION

There are several major aspects involved in designing
helicopters to crashworthiness specifications. First, a
knowledge is required of how crash impact energy is absorbed
and attenuated. For a helicopter in a typical crash this
impact energy would be absorbed by the collapsing of the
landing gear, the crushing of the floor structure, and the
stroking or crushing of the pilot's and passengers' seats.
At the same time the structure must remain rigid and retain
enough of its structural integrity to prevent roof, engines,
and heavy objects from collapsing upon the occupants. These
requirements are outlined and specified in great detail in

*
Captain D.C. Bannerman is presently performing research
at the DFVLR Stuttgart as part of a 2 year exchange program
with the U.S.A.F. Air Force System Command.

MIL-STD-1290 /1/, and the Crash Survival Design Guide /2/.
Of importance then is an understanding of the crash behav-
iour and energy absorption characteristics of the individu-
al structural elements.

Tubular elements are used extensively in several major
structural areas, landing gear, seat structures, and engine
mounts. Although tubes and welded sheet metal sections of
circular and rectangular cross sections have been studied
in the past (/3/,/4/, and /5/ for example); the studies were
generally intended for train or automobile applications. Also,
the studies were normally more theoretical in nature and tend
to be difficult to apply to design practices. Therefore a
series of tests was conducted for square and circular alu-
minum tubes with thickness to diameter ratios (t/D) varying
between .01 and .10 under quasi-static (20 mm/min) and impact
axial loading. Impact velocities varied to 12.8 m/s in ac-
cordance with MIL-STD-1290 /1/. The overall purpose for these
tests was to develop a basic understanding of the factors
affecting the energy absorption characteristics of tubular
elements while at the same time providing basic data accept-
able for design and analysis purposes. Also important is to
provide a baseline for comparison with separate composite
tube tests /6/.

The fuselage subfloor section is also important for the
absorption of crash impact energy. Here the energy is absor-
bed primarily through the crushing of the individual beam
elements. For this reason a series of tests was also conduct-
ed on beam sections of sandwich and stringer stiffened con-
struction. Composite sections as well as aluminium were test-
ed because of the increased usage of composites in primary
fuselage structures, as evidenced by the Advanced Composite
Airframe Program /7/. Test specimen geometries of the alu-
minium sections were selected to simulate typical subfloor
construction while at the same time providing for ease of
manufacture. The composite elements were then designed to
the same web shear strengths as the aluminium elements. Both
quasi-static and impact tests were performed and various me-
chanisms for producing stable, energy absorbant failures were
investigated. These tests were not intended to produce data
directly applicable to design since the actual beam geome-
tries would vary according to the design requirements, but
rather to provide a basic understanding of the crash behav-
iour of the individual elements. Also of prime importance
is the comparison of the composite energy absorption charact-
eristics to those of aluminium.

What follows is a discussion of the test results and
a comparison of the important energy absorption parameters
- load uniformity, stroke efficiency, average crush stress
level, and specific energy. As will be shown the composite
elements have surprisingly good energy absorption character-
istics and can be designed to produce as good as and general-
ly better performance than aluminium.

1. TEST SPECIMENS

1.1 Aluminium tubes

The aluminium tubes specimens were manufactured from square
and round Al Mg Si 0.2 F22 aluminium tubing with an ultimate
tensile strength of 226 MPa. In order to be pertinent to
normal aircraft applications the tubes had an inner dimens-
ion of 24 mm and the wall thicknesses varied from 0.25 mm to
3.0 mm, producing thickness to diameter ratios (t/D) of 0.01
to 0.10. The length of all tube specimens was 100 mm.

1.2 Stringer stiffened beam sections

As metal base lines, "U" shaped beam sections with
various stringer stiffener configurations were riveted to-
gether using 1 mm thick sheet aluminium bent to the proper
shape. Stiffener shapes were selected to represent simple
joint intersections as well as basic stiffener elements.
Composite stringer stiffened beam sections were then desig-
ned to similar shapes with the same or better shear-web
strengths. Stiffeners were initially bonded to the composite
"U"-sections but in initial tests the stiffeners simply de-
bonded. Therefore they were also riveted. The composite
stiffeners and "U"-sections were manufactured in steel mold
forms using a reusable silicone rubber core (Wacker Sili-
cone TRV-ME 622) which, when heated during the cure cycle,
expanded to provide proper curing pressure. Example test
specimens are shown in Fig. 1 and dimensions and materials
are given in Fig. 2.

1.3 Sandwich beam sections

To simplify construction, the aluminium and composite
sandwich beam specimens were fabricated in sections with a
"U"-shape similar to the stringer stiffened sections, using
the same materials and laminate lay ups. These "U"-shapes
were then bonded to Nomex or foam cores. Little attention
was paid to the beam cap design as it would normally be de-
signed to carry the required loads but contributes nothing
to energy absorption. Then to prevent the foam or Nomex
cores from simply splitting during loading, some composite
sandwiches were stitched together through the core using
Kevlar rovings. In some cases the core material did not
reach the full length of the section. This was to allow for
an early intitial deformation in the radius to propagate a
simple sinusoidal type buckle form. In other cases, an alu-
minium wedge was bonded in place at the radius to force a
debonding-rolling type of deformation. The success of these
techniques will be discussed later. Sample sandwich speci-
mens are shown in Fig. 3 and dimensions and materials are
given in Fig. 2.
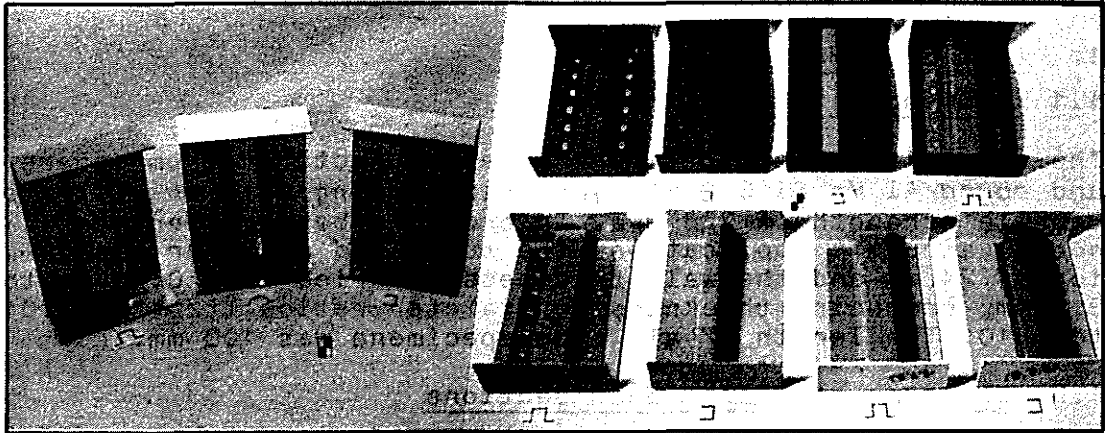
Fig.1 Aluminium (left) and composite (right) stringer stiffened elements.
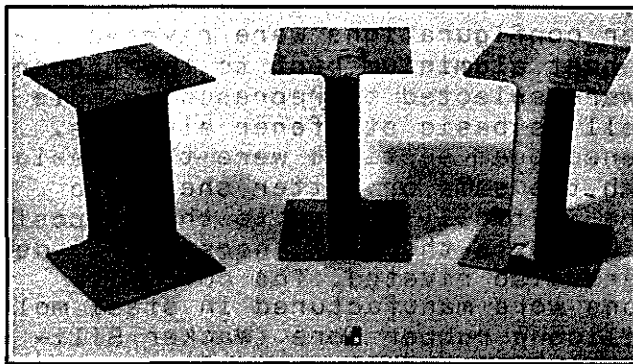
Fig.3 Sandwich elements.

STIFFENER, U-SECTION, and SANDWICH MATERIALS

ALUMINUM	KEVLAR	CARBON		RESIN	CORE		ADHESIVE
AL CU MG 1 F 40	INTERGLAS 98611 50% WARP	BROCHIER G 808 90% WARP	INTERGLAS 03040 50% WARP	BAKELITE L 20/SL 15hr at 80°C	HEXCEL HRH 10/OX (NOMEX)	ROHACELL 71 ACRYLIC FOAM	CIBA AW106/HV953U 7-12hr at R.T.

STIFFENER

U-SECTION

SANDWICH

(dimensions: STIFFENER 30, 20, 70×140; U-SECTION 150×100, 40; SANDWICH 100, 150×100, 20, STITCHING, WEDGE)

TEST SPECIMEN DATA

SPEC. NO.	LAMINATE LAY-UP			Wt. (g)	COMMENTS
	U-SECTION	STIFFENER			
AHUT	ALUMINUM	ALUMINUM	⊓	99	RIVETED TOGETHER
ARHUT	"	"	⌒	94	
AEL	"	"	⊏	85	
KHUT	$(\pm45^\circ_K,\pm45^\circ_K,0^\circ\text{-}90^\circ_K,0^\circ\text{-}90^\circ_K)_s$	$(\pm45^\circ_K,0^\circ_K)_s$	⊓	70	BONDED AND RIVETED TOGETHER
KEL	"	"	⊏	59	
KCHUT	$(\pm45^\circ_K,\pm45^\circ_K,0^\circ_C)_s$	"	⊓	69	
KCEL	"	"	⊏	60	
CKHUT	$(\pm45^\circ_C,\pm45^\circ_K,0^\circ_C)_s$	"	⊓	71	
CKEL	"	"	⊏	62	
CHUT	"	$(\pm45^\circ_C,0^\circ_C,0^\circ_C)_s$	⊓	71	
CEL	"	"	⊏	65	
ASW	ALUMINUM	(SANDWICH)	Ⅱ	220	
ASWT	"	"	Ⅱ	275	WEDGE
KSW	$(\pm45^\circ_K,\pm45^\circ_K,0^\circ\text{-}90^\circ_K,0^\circ\text{-}90^\circ_K)_s$	"	Ⅱ	171	STITCHED HORIZ.
KCSW	$(\pm45^\circ_K,\pm45^\circ_K,0^\circ_C)_s$	"	Ⅱ	147	IN CENTER
KCSWST	"	"	Ⅱ	220	STITCH SPACING
CSWST	$(\pm45^\circ_C,\pm45^\circ_C,0^\circ_C)_s$	"	Ⅱ	225	EVEN, WEDGE

Fig.2. Aluminium and composite stringer stiffened and sandwich element data.

2. TEST METHODS

All quasi-static tests were done in a standard tension/compression testing machine. The crosshead speed during compression was held at 2 mm/min until initial failure and was increased to a maximum of 20 mm/min for further deformation. All tests were done at room temperature and room humidity. A metal bolt was used to fix the tube specimens sidewards. The aluminium and composite stringer stiffened sections were bolted in place and the sandwich sections were fixed with double sided adhesive tape. The fixing was neccessary to prevent lateral motion, especially during the impact tests.

Impact tests were conducted in a drop test facility where weights of up to 60 kg can be dropped from heights to 16 m along a guide rail onto the test specimen. A decelerometer attached to the drop weight, emits a signal during impact. By integrating this deceleration-time signal, computer plots of velocity-time, deflection-time, force-deflection, and energy-deflection can be generated. This data was then used to calculate the various energy absorption parameters discussed later. Where applicable a linear regression analysis was performed to obtain the appropriate linear relations.

3. TEST RESULTS

3.1 Aluminium tubes

3.1.1 Failure modes

Typical crushed tubes both square and round are shown in Fig.4. Basically, there were two types of failure modes encountered with the square tubes; ring buckles, and alternating inside-outside folds. The transition point was at t/D equal to 0.065 for both static and impact tests. There were only two variations to this. One was for low t/D ratios (0.01) where the very thin wall thicknesses made the specimen sensitive to manufacturing and loading imperfections, resulting in an irregular collapse. The other was for t/D ratios greater than 0.08 under impact loading where the tube split along each of the corners and the four sides simply rolled up. As will be evident later, the irregularities produce variations in the energy absorption characteristics.

The round tubes had failure modes similar to the square tubes; ring buckles, diamond shaped buckles, and combinations of the two. They were, however, not as regular as the square tubes and a transition point between the two basic buckling shapes was not as readily evident. For example, Fig.4 shows that for t/D = 0.03 the failure mode was completely diamond shaped buckles. However, for impact loading, specimens failed in a completely ring buckling shape (similar to that for t/D = .045 in Fig.4) as well as in a completely diamond buckling shape. This lack of consistency produced more scatter in the data as compared to the square tubes.
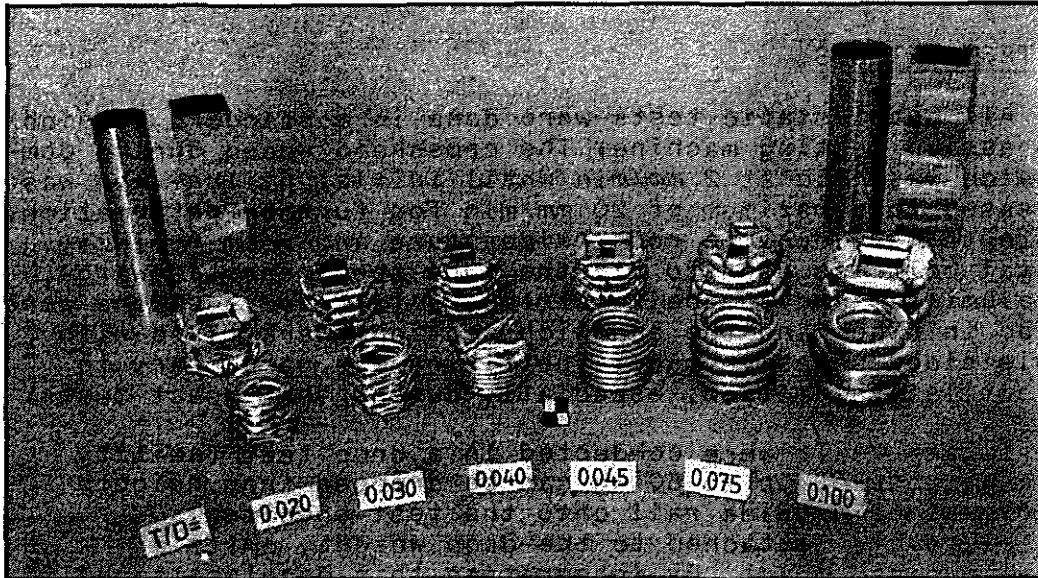
Fig.4. Typical failure modes for round (front) and square (back) aluminium tubes under quasi-static loading.

These failure modes are identical to those obtained by Alexander /3/, Pugsley and Macauley /8/, and others (4, 5, 9, 10), who have discussed the mechanics and analysis of the various shapes in great detail. It is therefore not necessary to discuss them further here.

3.1.2 Energy absorption properties

The basic parameters describing the crush energy absorption properties to be discussed here are load uniformity, stroke efficiency, average crush stress, and specific energy. The load uniformity is the ratio of the highest peak load (usually the initial buckling load) to the average crushing load. The lower the load uniformity is the better it is for the helicopter occupants because it means a smoother deceleration. Load uniformity values for round and square tubes are plotted in Fig.5 along with several composite tube results /6/ for comparison. The initial rise in load uniformity for the square tubes is a result of the increase in buckling load with the thickness. The drop off in load uniformity for both round and square tubes is a result of the increased amount of material undergoing plastic deformation and the accompanying rise in average crush stress levels (See Fig. 7 and 9).

The stroke efficiency, Fig.6, is a measure of how efficient the failure mode is in collapsing together. The higher the value is, the more efficient the absorber is. Obviously, the thicker the tube is the more material there is to compact together and the stroke efficiency should naturally decrease. This is quite evident with the round tubes,
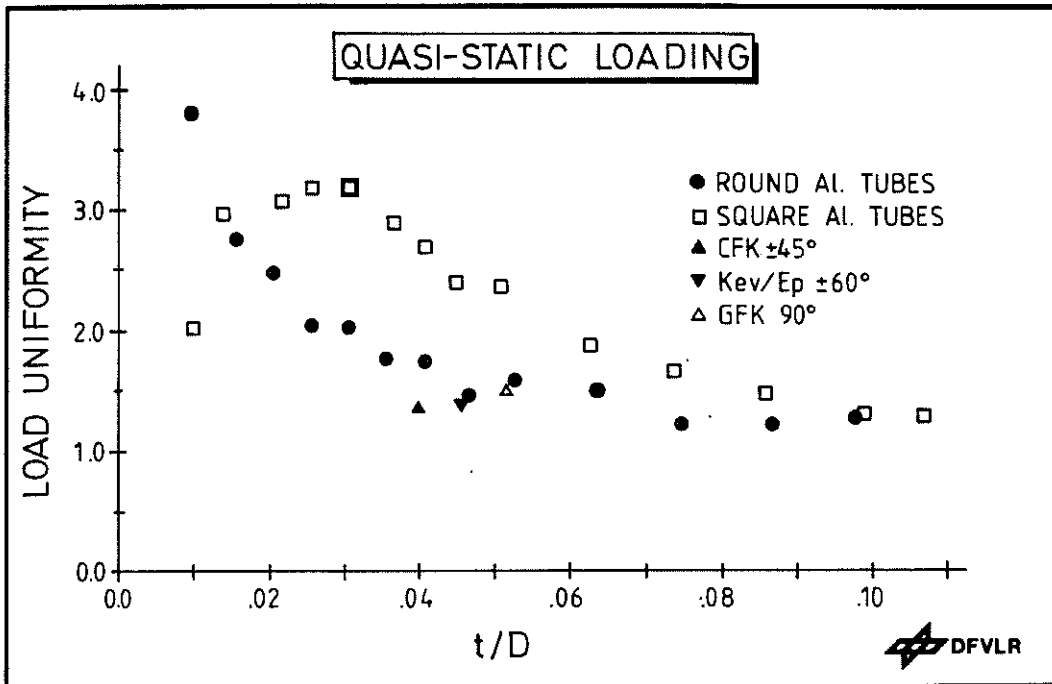
Fig.5. Load uniformity vs. t/D for round and square aluminium tubes and round composite tubes /6/.
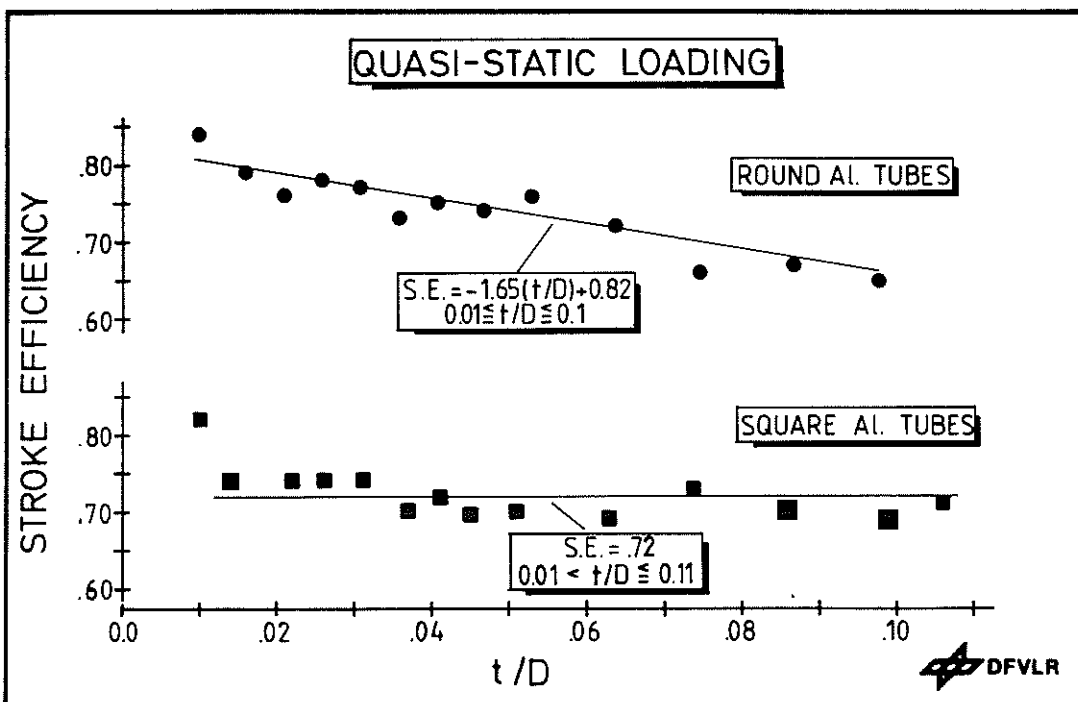
Fig.6. Stroke efficiency vs. t/D for round and square aluminium tubes.

as shown by the upper curve in Fig.6, which was found to be linear. The decrease in stroke efficiency for square tubes, although evident, was found to be small enough that the stroke efficiency could be assumed constant for this range of t/D values. The high value at t/D = .01 is a result of the irregular collapse mode for this tube as mentioned earlier in section 3.1.1. It was therefore omitted for further analysis, but nonetheless included on the various graphs to show that it did have comparable energy absorption properties.

The average crush load is obtained by dividing the absorbed energy by the stroke length. From this the average crush stress is easily calculated by dividing by the cross sectional area. Then to characterize the results with a material property, the average stress is normalized by dividing by the ultimate tensile strength. The results are plotted in Fig.7 for square tubes and in Fig.9 for round tubes. Using a linear regression analysis, the relation between stress ratio and t/D was found to be linear for both square and round tubes. For different materials, this relation will remain linear but have respectively different constants. (To verify this simply plot the results obtained by Alexander /3/, Pugsley and Macauley /8/, or Johnson et al /9/).

The specific energy is obtained by dividing the actual absorbed energy by the mass of the test specimen. These values are plotted in Fig.8 for square tubes and Fig.10 for round tubes. Since it is evident that the stress ratio is predominately linear, specific energies for material with similar properties could also be calculated. The average crush stress and specific energy can be defined in equation form as

$$\sigma_{avg.} = E / (l \cdot A) \qquad\qquad E_s = E / m$$

Where E is the actual absorbed energy, l is the stroke length, A is the cross-sectional area, and m is the specimen mass. Noting that the mass and stroke efficiency (SE) can be expressed as

$$m = \rho \cdot L \cdot A \qquad\qquad SE = l / L$$

Where ρ is density and L is specimen length, the above equations can be combined to obtain

$$E_s = (SE \cdot \sigma_{avg.}) / \rho$$

Since the stroke efficiency and the average crush stress have both been shown to be linear with respect to t/D, E_s can also be plotted as a simple function of t/D. These curves for E_s are plotted in Figs.8 and 10 using the linear relations for stroke efficiencies and stress ratios given in Figs.6, 7 and 9. Since the stroke efficiency for square tubes was found to be basically constant E_s versus t/D for square tubes should also be linear. This was verified by
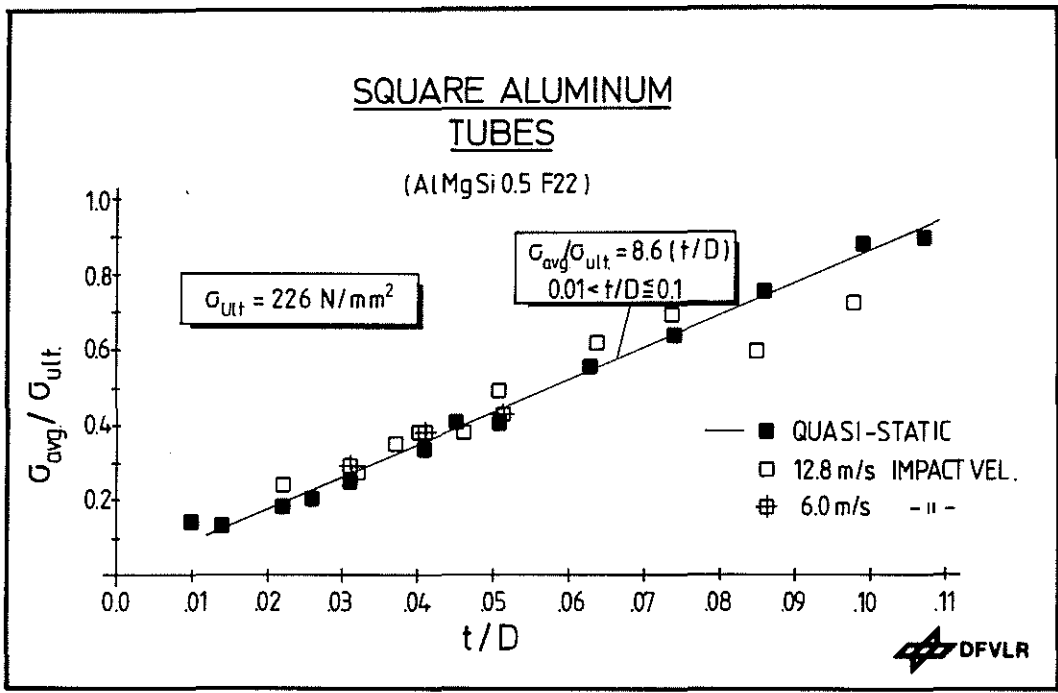
Fig.7. Average crush stress to ultimate tensile stress ratio vs. t/D for square aluminium tubes.
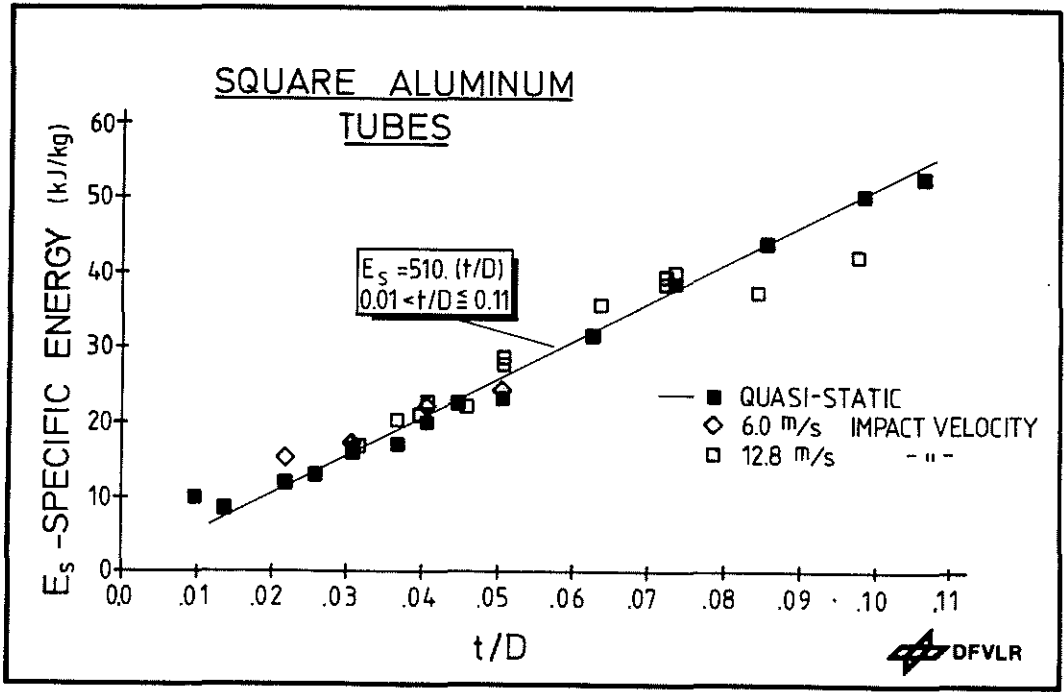
Fig.8. Specific energy vs. t/D for square aluminium tubes.

ROUND ALUMINUM TUBES

(AlMgSi0.5 F22)

$\sigma_{ult} = 226 \text{ N/mm}^2$

$$\frac{\sigma_{avg}}{\sigma_{ult}} = 8.28\,(t/D) + 0.16$$
$$0.01 \leqq t/D \leqq 0.1$$

— ● QUASI-STATIC
○ 12.8 m/s IMPACT VELOCITY
△ 9.0 m/s — '' —
⊕ 6.0 m/s — '' —

DFVLR
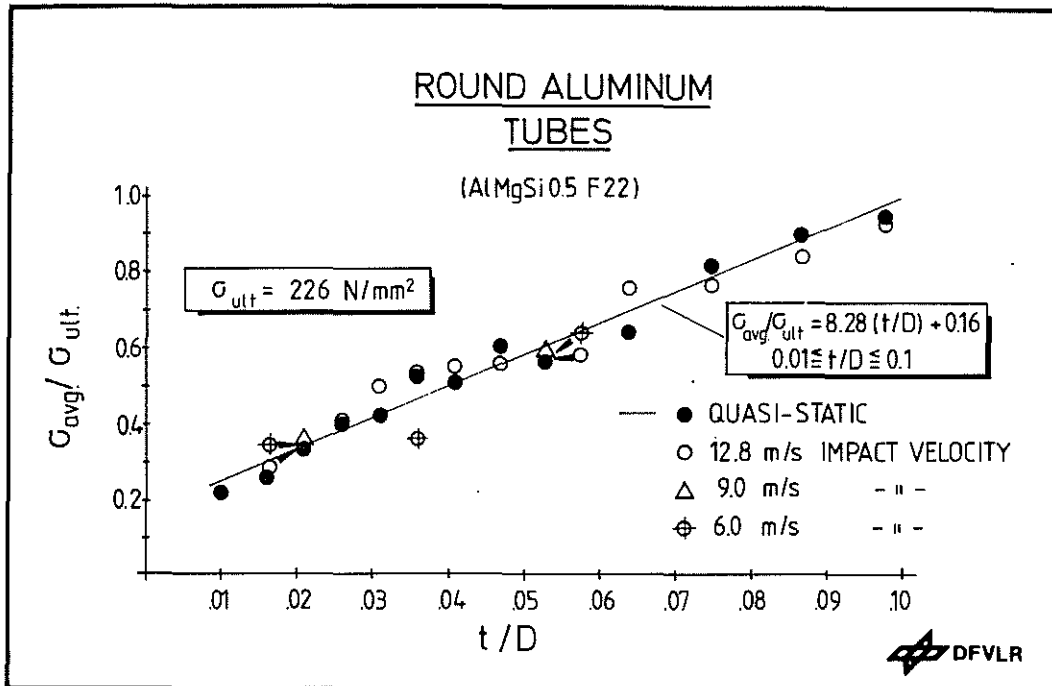
Fig.9. Average crush stress to ultimate tensile stress ratio vs. t/D for round aluminium tubes.

ROUND TUBES

$$E_S = -1143\,(t/D)^2 + 548\,(t/D) + 11$$
$$0.01 \leqq t/D \leqq 0.1$$

	quasi-static	6.0 m/s	9.0 m/s	12.8 m/s IMPACT VELOCITY
ALUMINUM	●	○	◇	□
CFK ±45°	▲	△		
Kev/Ep ±60°	▼	▽		
GFK 90°	●	○		

DFVLR
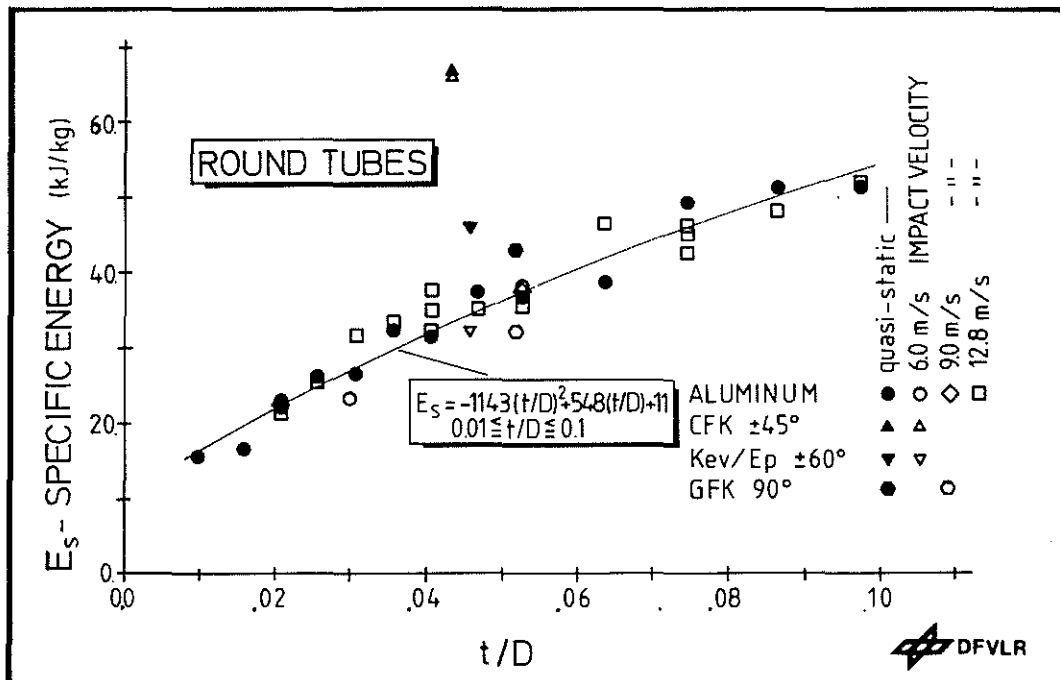
Fig.10. Specific energy vs. t/D for round aluminium and composite /6/ tubes.

performing a regression analysis on the actual specific
energy data which resulted in a linear relation almost ident-
ical to that found using the above equations. The second order
curve calculated for the round tube specific energies also
fits the data quite well.

The effect of impact loading was generally relatively
small. It could be argued that the average crush stress and
specific energy levels are slightly higher for impact tests
but the differences are so minor for the velocities tested
that static and impact results can be assumed equal. The
only major difference was for square tubes with t/D > 0.08
where impact loading caused a different failure mode to
occur, resulting in lower specific energies.

It is interesting to point out here that the results
for composite tubes /6/ shown in Figs.5 and 10 are generally
better than these for the aluminium tubes.

3.2   Stringer stiffened beam sections

3.2.1   Failure modes

Several typical crushed beam sections are shown in
Fig.12. As was expected from tube and pretest results, the
carbon sections exhibited a tendency to fail in a global frac-
ture mode. The panel sections tended to fold into large,
irregular, unsymmetric shapes and fracture completely at each
fold line. The carbon hat stiffener sections failed in a
more regular rolling up manner, fragmenting into small
pieces as it rolled. This resulted in higher crush load val-
ues of energy absorption. Deformation began in the radius
between the panel and flange sections and progressed smooth-
ly into the stiffener, helping to produce the stable stiff-
ener failure mode described above. It also helped to remove
the high initial peak loads experienced with tubes. The open
"U"-section stiffeners exhibited simple column-panel buckling
as a result of their lower cross sectional stiffness. Un-
fortunately, the carbon panels generally fractured into
large pieces which scattered in all directions, introducing
instabilities and load direction sensitivities. For this
reason Kevlar and Kevlar/Carbon hybrids were tested.

As is evident in Fig.11, Kevlar improves the basic
structural integrity of the elements considerably. They
still remain in one piece after the test. As the amount of
Kevlar was increased, the fold and buckle sizes became
smaller and more regularly spaced. For the Kevlar panel
section-hybrid hat stiffener combination (KHUT in Fig.2),
the panel deformed in a very regular, sinusoidal type folding
pattern until the material became too compacted, forcing it
into a simple buckling shape. The completely hybrid element
(KCHUT in Fig.2) deformed similarly but the patterns were
larger and more irregular in shape.

Generally, the composite closed hat shape stiffened elements were more stable and energy efficient than the open "U"-shape stiffened elements. These open stiffener elements tended to buckle in a simple column-panel buckling form and then collapse under further loading. Average crushing loads were then lower. This was opposite to that found for the aluminium elements. The "U"-shaped aluminium stiffeners failed in a rolling up manner, tearing along the bend radius, while the square hat stiffened elements experienced typical column buckling failures. The aluminium round-hat stiffend panels were unique in that the initial bending motion begun in the upper and lower flange radii continued into the stiffener producing a rolling-fragmenting type failure.

3.2.2 Energy absorption properties

The average crush force levels (F_{avg}), load uniformities (L.U.), and specific energies (E_s) are shown in Fig.13 for the various stiffened beam sections described in Fig.2. The better values are for load uniformities approaching unity and higher specific energies. As is evident, the composite elements fit these requirements quite nicely and compare very favorably with aluminium. As a result of the initial flange radius deformation described earlier, the material began to fail at load levels which although relatively high, were lower than the buckling loads. This produced lower load uniformities. It also helped initiate the smoother, more stable, energ absorbing failure modes and resulted in the higher specific energies. The open shaped stiffeners had lower buckling strengths which were quickly reached in the crushing process. After which the average force levels were relatively low, producing high load uniformities and lower specific energies.

The carbon hat elements (CHUT) displayed the best characteristics. But, as mentioned earlier, they tended to fracture catastrophically and were load direction sensitive. This is evident by the large drop in specific energy for impact loading where the axial loading can not be as accurately controlled. On the other hand, the Kevlar sections (KHUT) experienced a similar drop in specific energy with impact loading. This was because the speed of the impact deformation did not allow the formulation of regular, even fold patterns obtainable in static tests. However, the hybrid elements (KCHUT) combine the high energy absorption properties of the carbon fibers with the stabilizing effects of Kevlar, producing practically identical impact and static characteristics. They also retain their basic structural integrity, have specific energies and load uniformities better than the tested aluminium elements and are roughly 30 % lighter than the aluminium elements.
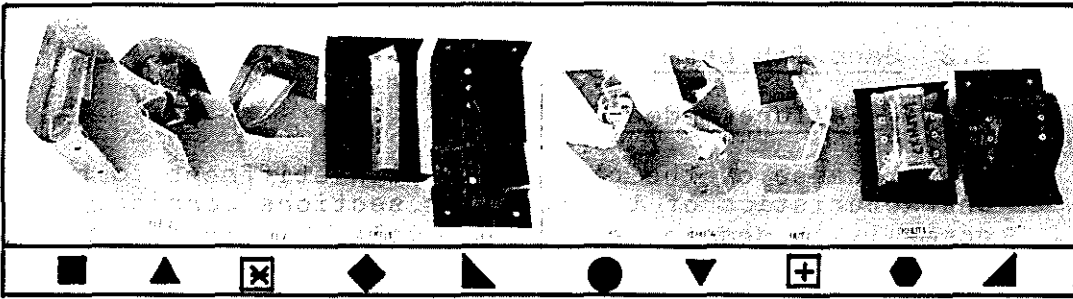
Fig.11. Typical stringer element failure modes.
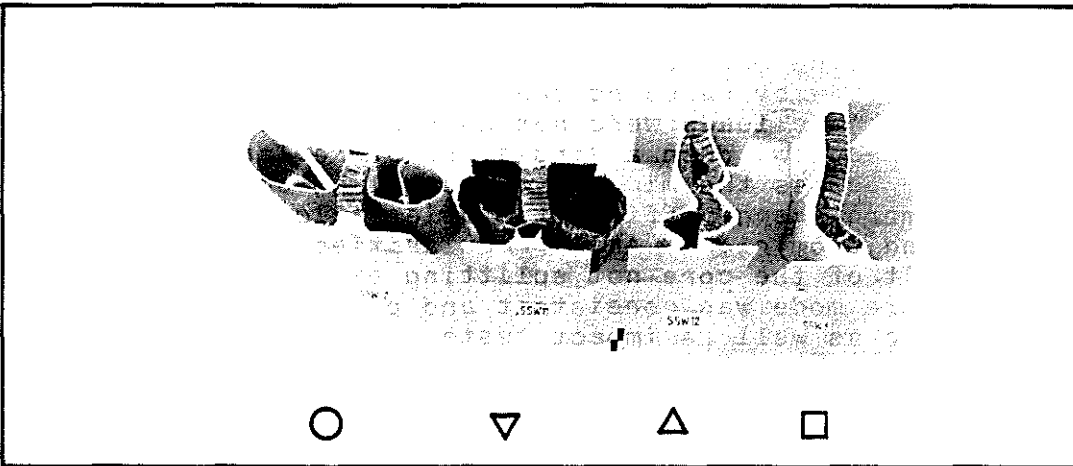
Fig.12. Typical sandwich element failure modes.

		TEST			DATA		
S Y M B O L	SPEC. NO.	STATIC			IMPACT		
		F_{avg} (N)	L.U.	E_{sp} (kJ/kg)	F_{avg} (N)	L.U.	E_{sp} (kJ/kg)
⊠	AHUT	2680	8.4	3.0	3020	7.3	3.4
⊚	ARHUT	7110	3.4	8.4	8090	3.3	9.7
⊞	AEL	3630	3.4	4.8	2760	5.6	3.6
■	KHUT	8890	2.0	14.3	5290	2.4	8.5
●	KEL	1420	6.0	2.7	--	--	--
▲	KCHUT	6220	2.2	10.4	6800	2.1	11.0
▼	KCEL	4890	2.4	9.1	2180	4.4	4.1
◆	CKHUT	5250	3.5	8.2	7380	2.7	12.0
●	CKEL	1200	7.3	2.3	1560	4.8	2.8
◣	CHUT	10940	2.3	17.6	7470	3.0	11.7
◢	CEL	1910	6.8	3.3	--	--	--
□	ASW	1890	12.0	1.0	--	--	--
○	ASWT	2710	12.4	1.1	2400	26.7	1.0
△	KSW	5740	2.4	3.9	6940	2.8	4.4
◸	KCSW	--	--	--	2730	5.0	2.0
◿	KCSWST	3690	8.6	1.9	2530	27.3	1.4
▽	CSWST	6850	6.3	3.4	4360	12.5	2.2

Fig.13. Test results for stringer and sandwich elements.

3.3 Sandwich beam sections

3.3.1 Failure modes

Because of the relatively high stiffness to height characteristics of the sandwich sections considered, they normally tended to fail in a simple buckling mode. A typical buckling failure is shown on the right in Fig.12 for an aluminium section. Also found was a ballooning type buckling where the Nomex or foam core split up the middle. When a portion of the core at the bottom was removed, the web radii were allowed to roll together, initiating a more steadily progressing onslaught to buckling. This improved the load uniformity by reducing the initial buckling loads but since the average loads were not increased the specific energies remained low. When a single row of Kevlar stitchings were added across the middle, the buckling shape was altered to the more energy efficient double balloon shown in Fig.12, second from right. Any irregularities in the shape are a result of the core not splitting exactly up the middle. This failure mode was consistent and produced similar results for static as well as impact tests.

The use of a wedge at the bottom combined with a reduced bonding area in the flanges produced the failure mode shown at the left in Fig.12. Guided by the wedge, the aluminium web skin simply rolled up. However, after initial debonding, the composite web cores split up the middle and bending occured in the upper flange radii. The web skins remained relatively flat. The addition of stitchings evenly spaced throughout the web stabilized the failure mode into one similar to the aluminium (second from left in Fig.12). In addition to the core crushing and web skin rolling-fracturing, energy was absorbed through the tension failure of the Kevlar stitches.

3.3.2 Energy absorption properties

The normal buckling failure modes have generally poor energy absorption properties. High buckling loads and low post buckling load levels are the causes. The removal of a portion of the core along with the addition of a single horizontal row of stitches improved on both of these factors. The results are given in Fig.13 for test specimens KSW and KCSW. They show a considerable improvement over the basic aluminium sandwich, ASW. The sandwich properties could also be further improved by varying core.and skin thickness along with the number of rows of stitches.

The use of the wedge with evenly spaced stitches also improved the specific energies to values better than those obtained for aluminium. Load uniformities were also reduced but still remained relatively high. The peak load, however, could be reduced by reducing the bond areas of the flanges. The weight of the wedge was included in the calculations for

comparison purposes and accounts for up to 25 % of the total
weight. The specific energy would be correspondingly increas-
ed if the wedge shape was designed into the beam caps in a
manner similar to that used in the Boeing 234 helicopter sub-
floor beams /11/. This stitching and wedge mechanism was not
as energy efficient as that described in the previous para-
graph. In comparison though, a carbon sandwich being more
brittle will not produce the even folding deformation ob-
tained with the Kevlar sandwich. In which case this method
would be more efficient.

CONCLUSION

Square and round aluminium tubes with t/D ratios between
0.01 and 0.10 were tested under quasi-static and impact axial
loading. The tube configurations and properties were such
that they could be applied as helicopter or aircraft seat
and landing gear load carrying members and additionally
serve as energy absorbing devices. Failure modes are consist-
ent and regular. Ring buckles, alternating inside outside
folds, and diamond shaped buckles occur. These failure modes
are natural and require no trigger mechanisms to initiate
and stabilize the energy absorbing crushing.

The energy absorption properties were found to be de-
pendent on the t/D ratio. For stroke efficiency, average
crush stress, and specific energy for square tubes, this re-
lation is linear. But for the specific energy of round tubes,
it is a second order function. In general, average crush
stress and specific energy increase with increasing t/D ratio
as a result of the increased amount of material undergoing
plastic deformation. In comparison with composite tubes, how-
ever, the specific energy and load uniformity for aluminium
tubes are not as good.

The aluminium elements were selected to simulate typical
subfloor elements and the composite elements were designed
to imitate them in size, shape, and strength properties.
Within these guidelines, it was found that by proper selec-
tion of materials (Kevlar/carbon hybrids) along with the addi-
tion of simple failure triggering and stabilizing mechanisms,
consistent and efficient energy absorption properties can
be produced. These properties were found to be as good as
and generally better than their aluminium counterparts. Also,
they can be further improved and optimized within the restric-
tions of aircraft structural requirements by varying the degree
of hybridization, lay-up sequence, number of laminates, and
fiber orientations, as well as by refining the failure trigger
mechanisms further, and by varying the shape of the structural
elements.

REFERENCES

1) Military Standard, MIL-STD-1290 (AV), "Light Fixed- and Rotary-Wing Aircraft Crashworthiness", Department of Defense, Washington, DC, 25 January 1974.

2) "Aircraft Crash Survival Design Guide", USARTL TR-79-22, Volumes I through V, Applied Technology Laboratory, USARTL (AVRADCOM), Fort Eustis, Virgina, 1980.

3) J.M. Alexander: "An Approximate Analysis of the Collapse of Thin Cylindrical Shells Under Axial Loading." Quart. Journ. Mech. and Applied Math. Vol.XIII, Pt 1, 1960, pp 10-15.

4) R.C. VanKuren and J.E. Scott: "Energy Absorption of High-Strength Steel Tubes Under Impact Crush Conditions." Society of Automobile Engineers Paper No. 770213, 1977.

5) Norimoto Aya and Kunihiro Takahashi: "Energy Absorbing Characteristics of Vehicle Body Structure (Part 1)." Bulletin of JSAE, No 7, pp 65-74, 1976.

6) C.M. Kindervater: "Energy Absorbing Qualities of Fiber Reinforced Plastic Tubes." Presented at the American Helicopter Society National Specialists' Meeting on Composite Structures, Philadelphia, Pennsylvania, March 23-25, 1983.

7) Brian L. Carnell and Mukunda Pramanik: "ACAP Crashworthiness Anlaysis by KRASH." Presented at the American helicopter Society National Specialists' Meeting on Composite Structures, Philadelphia, Pennsylvania, USA, March 23-25, 1983.

8) Sir Alfred Pugsley and M. Macaulay: "The Large Scale Crumpling of Thin Cylindrical Columns." Quart. Journ. Mech. and Applied Math. Vol.XIII, Pt 1, 1960, pp 1-9.

9) W. Johnson, P.D. Soden, and S.T.S. Al-Hassani: "Inextensional Collapse of Thin-Walled Tubes Under Axial Compression." Journal of Strain Analysis, Vol.12, No 4, 1977, pp 317-330.

10) Y. Ohkubo, T. Akamatsu, and K. Shirasawa: "Mean Crushing Strength of Closed-Hat Section Members." Society of Automotove Engineers Paper No 740040, 1974.

11) Leonard J. Marchinski and Robert L. Pinckney: "The Design, Construction, and Performance of Composite Fuselage Components for the Boeing 234 Helicopter." Proceedings of the 13th National SAMPE Technical Conference, October 13-15 1981, Mount Pocono, USA, pp 287-297.